Corrosion inhibition of carbon steel by acridine orange in HCl solution: Electrochemical and weight loss studies

Aboozar Taheri* & Hossein Ahmadi

Department of Chemistry and Chemical Engineering, Lamerd Branch, Islamic Azad University, Lamerd, Iran

E-mail: ab.taheri@iau.ac.ir

The inhibition effect of acridine orange (AO) on the corrosion of A105 carbon steel in 0.5 M hydrochloric acid has been investigated using potentiodynamic polarization, electrochemical impedance spectroscopy (EIS) and weight loss tests. Using polarization plots and corrosion rate calculations, it has been revealed that AO acts as an effective inhibitor. The results have showed that the inhibition efficiency increases with increasing inhibitor concentration and A behaves as a mixed type inhibitor in HCl solution. Based on the data obtained from the EIS tests, it has been determined that the charge transfer resistance increased from 74.20 $\Omega.cm^2$ for blank solution to 250 $\Omega.cm^2$ for 100 ppm of AO. Comparison of the results obtained from the three methods, have shown that the methods are in acceptable agreement. Investigation the effect of temperature in the range of 20-60 °C has indicated that the inhibition efficiency increased with temperature, so that at 40 and 60 °C, the inhibition efficiency would reach 90%. The thermodynamic parameters of steel dissolution including activation energy, standard enthalpy and entropy of activation have been calculated and discussed. It was also found, that the adsorption of AO on the steel surface has obeyed Langmuir isotherm and adsorption has been performed spontaneously.

Keywords: Acridine orange, Carbon steel, Corrosion, Electrochemical tests, Inhibitor, Weight loss

Steel and its alloys are mainly used in the construction of tanks, oil and gas refinery equipment, pipelines, etc. The main problem of using steel alloys is their corrosion in acidic solutions[1]. According to the National Association of Corrosion Engineers, the cost of corrosion in different countries is about 1-5% of their gross national product[2].

Acid solutions, such as hydrochloric acid and sulfuric acid, are commonly used to remove unwanted deposits and corrosion products in many industrial processes[1]. Even if the duration of exposure to acid is very short, these acidic media are highly corrosive to steel materials[3]. Corrosion inhibitors are often used in these processes to control the dissolution of iron and iron alloys[4]. Therefore, the development of highly efficient, low cost and low toxicity organic corrosion inhibitors is essential for such industrial applications[3].

The presence of heteroatoms such as N and O and multiple bonds in the compound structure increases the electron density of the inhibitor and allows the formation of a bond between the inhibitor and the metal[5]. Dyes are a group of organic compounds that have such properties and can act as effective corrosion inhibitors.

Hitherto, several studies have been conducted on the corrosion inhibitory properties of organic dyes. For instance, neutral red (NR)[6], thymol blue[7,8], bromophenol blue[8], Congo red[9,10], methylene blue[11,12], methyl green[13], crystal violet[14], methyl orange[15], methyl violet[16, 17], Alizarin violet 3B[18] and acid violet 6B[19] have been used as corrosion inhibitors for various steels in HCl and H_2SO_4 environments. However, information on the use of organic dyes as corrosion inhibitors is still scarce and further studies are needed. Acridine orange (AO) (Figure 1) is a basic fluorescent dye whose structure is based on the heterocyclic skeleton of acridine[20].

In the present study, the inhibition effect of acridine orange on corrosion of A105 carbon steel (CS) in 0.5 M HCl medium was investigated by
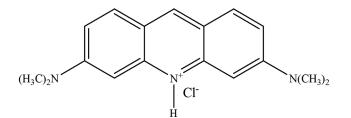

Fig. 1 — Molecular structure of acridine orange.

Table 1 — Chemical composition of A105 carbon steel[21].

Element	C	Mn	P	S	Si	Cu	Ni	Cr	Mo	V
Weight%	0.35	0.6-1.05	0.035	0.04	0.1-0.35	0.4	0.4	0.3	0.12	0.08

electrochemical polarization, electrochemical impedance spectroscopy (EIS) and weight loss measurements.

Experimental Section

Chemicals and solutions

Acridine orange zinc chloride double salt, 37% hydrochloric acid and ethanol were purchased from Merck, Germany and used with no further purification. Inhibitor solution with a concentration of 500 ppm was prepared by dissolving AO salt in ethanol. This solution was used as the stock inhibitor solution and an appropriate volume of that was added directly to 0.5 M HCl solution to prepare the desired concentration in range from 5 to 100 ppm. Aggressive solution of 0.5 HCl M was prepared by diluting 37% hydrochloric acid with doubly distilled water.

Preparation of steel specimens

In this study, a sample of A105 CS with the chemical composition given in Table 1 was used. It is categorized as medium carbon steel that is used in the manufacture of pipes to transport oil, gas and water in the oil and gas and petrochemical industries.

For gravimetric measurements, the CS specimens with a rectangular form of $0.4 \times 1 \times 1$ cm^3 were prepared by laser cutting. Similar samples were prepared for electrochemical measurements, except that here the sample was connected to a copper wire and embedded in epoxy resin with anexposed surface area of 1 cm^2. The later samples were used as working electrodes in the electrochemical experiments. Prior to all measurements, the specimens were polished successively with 200 to 1200 grades of silicon carbide abrasive paper, followed by cleaning with doubly distilled water and acetone.

Weight loss studies

Pre-prepared A105 CS specimens were carefully weighed and immersed in 100 mL of corrosive solution with different inhibitor concentrations at 20 °C for 24 h. After this time, the samples were taken out, immersed in sulfuric acid M 1 for 1 minute, the steel surface was cleaned with a soft brush and finally rinsed with distilled water to remove corrosion deposits from the steel surface. The samples were

weighed again after drying. In order to obtain good repeatability, each experiment was repeated three times and their results were averaged. Corrosion rate (CR, $mgcm^{-2}h^{-1}$) and inhibition efficiency ($\eta\%$) were calculated usingthe following equations[22]:

$$CR = \frac{\Delta w}{S.t} \qquad \ldots (1)$$

$$\eta\% = \frac{C_R^0 - C_R}{C_R^0} \times 100 \qquad \ldots (2)$$

where Δw, s, t, C_R and C_R^0 are weight loss (average) of specimen (mg), area of the specimen (cm^2), immersion time (h), and corrosion rates of CS samples in the electrolyte solution with and without inhibitor, respectively. The corrosion rates obtained from Eq. (1) is converted to the mpy scale as follows:

$$CR_{mpy} = \frac{534\Delta w}{DAt} \qquad \ldots (3)$$

where D and A are the density of the steel sample (gcm^{-3}) and area of the specimen (in^2) and Δw and $t$have the same meaning as before.

Electrochemical measurements

All electrochemical experiments were performed using an AUTOLAB potentiostat/galvanostat (model PGSTAT204) with FRA32M module controlled by NOVA software. A conventional three-electrode glass cell was used for polarization and EIS measurements which consisting of a CS specimen, a platinum rod and a saturated calomel electrode (SCE) as working (WE), auxiliary and reference electrodes, respectively.

All experiments were performed in quiescent solution. Before each polarization and EIS experiments, the working electrode was immersed in 25 mL of the test solution for 60 minutes to obtain the open circuit potential (E_{OCP}). Potentiodynamic polarization curves were recorded by automatically scanning the potential in the range of $E_{OCP} \pm 250\,mV$ versus SC Eat a scan rate of $1mVs^{-1}$. EIS measurements were conducted using AC signals of 10 mV of amplitude, in the frequency range of 100 kHz to10 mHz after establishing the E_{OCP}.The experiments were performed at constant temperatures

of 20, 40 and 60 °C by temperature control by water bath without inhibitor and with 5-100 ppm of the AO in 0.5 M HCl. Measurements were repeated at least three times to ensure repeatability of test results.

Corrosion current density (j_{corr}), corrosion potential (E_{corr}) and corrosion rate (CR) values wereobtained by NOVA software, and inhibition efficiency ($\eta\%$) of the inhibitor was determined as follows[23]:

$$\eta\% = \left(\frac{j_{corr}^0 - j_{corr}}{j_{corr}^0}\right) \times 100 \qquad \ldots (4)$$

where j_{corr}^0 and j_{corr} are corrosion current density in the absence and presence of the inhibitor, respectively. The degree of surface coverage (θ) was evaluated from the polarization curves[24].

$$\theta = \frac{\eta\%}{100} = 1 - \frac{j_{corr}}{j_{corr}^0} \qquad \ldots (5)$$

Results and Discussion

Polarization tests

Figure 2 illustrates the Tafel polarization curves of A105 steel sample immersed in 0.5 M hydrochloric acid solution in the absence and presence of various
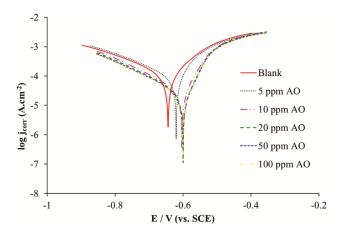

Fig. 2 — Potentio dynamic polarization curves for CS in 0.5 M HCl without and with different concentrations of AO at 20°C (immersion time is 60 min).

concentrations of AO at 20 °C. As can be seen, at concentration of 5 ppm of AO there was no obvious change in the Tafel curve with respect to blank, but from 10 ppm onwards, the curves were significantly shifted towards lower current density, indicating creating corrosion inhibition conditions. It can also be seen from the figure that the corrosion potential has shifted to more positive values. The potentiodynamic polarization data, corrosion rates, inhibition efficiency, and surface coverage at different inhibitor concentrations are listed in Table 2. From the results it is realized that added AO lessened the corrosion rate. Itis evident also that when the concentration of AO is less than 20 ppm, $\eta\%$ increases sharply with an increase in concentration, while a further increase causes no appreciable change in performance. According to Caldona et al.[25] report, because the largest shift in E_{corr} was smaller than ±85 mV relative to the E_{corr} of the blank solution the proposed inhibitor can be classified asa mixed type inhibitor. However, the positive E_{corr} shift in the presence of inhibitor indicatesthat AO can inhibit acid corrosion of carbon steel with predominantly control the anodic reaction[26].

Electrochemical impedance spectroscopy

Figure 3 shows the Nyquist diagrams of carbon steel in 0.5 HCl solution in the absence and presence
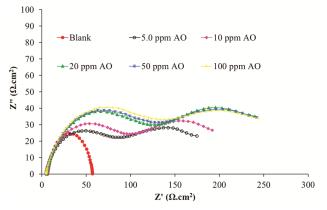

Fig. 3 — Nyquist plots for carbon steel in 0.5 M HCl at 20°C in the absence and presence of different concentrations of AO.

Table 2 — Potentiodynamic polarization parameters for the corrosion of CS in 0.5 M HCl containing various concentrations of AO at 20 °C.

AO concentration (ppm)	E_{corr}(V, vs. SCE)	β_a (V.dec^{-1})	β_c (V.dec^{-1})	R_p ($\Omega.cm^{-2}$)	j_{corr} ($mA.cm^{-2}$)	CR (mpy)	$\eta\%$	θ
Blank	-643	397	310	235.88	320	146.769	------	------
5	-620	330	288	248.72	269	123.133	16.04	0.160
10	-603	141	211	455.52	81	37.009	74.77	0.748
20	-614	134	191	549.85	62	28.494	80.57	0.806
50	-601	144	190	571.69	62	28.487	80.58	0.806
100	-601	152	1910	590.28	62	28.409	80.63	0.806

of different concentrations of AO inhibitor at 20 °C. As can be seen, the Nyquist diagram in the absence of the inhibitor contains a depressed semicircle with the center under the real axis, which is characteristic of solid electrodes and is due to geometrical factors such as roughness and in homogeneities of electrode surface[27].

In the presence of inhibitor, Nyquist plots consist of two time constants; the first loop, which appears at high frequencies, is related to charge transfer resistance, and the second loop, at low frequencies, can be due to th e adsorption of inhibitor molecules on the metal surface, which prevents the penetration of ions[28].As can be seen, the diameter of the semicircles has increased with increasing concentration of the inhibitor, which indicates an increasing inhibition of the charge transfer process at the metal-solution interface in the presence of the inhibitor[29].

Impedance spectra were investigated by fitting to the equivalent circuit model. Figures 4a and 4b show the equivalent circuits in the absence and presence of the inhibitor, respectively. In these circuits, R_s represent the solution resistance, R_{ct} is the charge transfer resistance, CPE_{dl} denotes the constant phase element related to the double layer capacitance, R_{ads} and CPE_{ads} are resistance and constant phase elements due to adsorption of AO molecules on the steel surface, respectively.

The double layer capacitance (C_{dl}) for a circuit containing CPE,can be calculated as follows[30]:

$$C_{dl} = (Y_0 R_{ct}^{1-n})^{\frac{1}{n}} \qquad \qquad \dots (6)$$

where Y_0 $(\Omega^{-1} cm^{-2})$ is the coefficient of CPE and n is the phase shift parameter whose value is between 0 to 1 and signifies interface surface properties of working electrode. Related impedance parameters obtained from the equivalent circuits are given in Table 3. Equation 7 was used to calculatethe inhibition efficiency (%)[31]:

$$\eta\% = \left[1 - \frac{R_p}{R_{p(i)}}\right] \times 100 \qquad \qquad \dots (7)$$

where R_p (sum of R_{ct} and R_{ads}) and $R_{p(i)}$, respectively, represent the polarization resistance in the absence and the presence of different concentration of inhibitor.

Results from Table 3 depict that R_s is almost constant in all experiments and only slightly decreases in the presence of AO inhibitor due to increased electrical conductivity as a result of the dissolution of dye salt in solution. On the other hand, R_{ct} increased sharply with increasing AO concentration up to 20 ppm and after that showed a slow increase. It is also observed that the double layer capacitance (C_{dl}) in the presence of AO has decreased compared to the blank. In the presence of AO, an additional resistance is formed in the solution due to the adsorption of AO on the surface of carbon steel (R_{ads}). This resistance also increases with increasing AO concentration up to 20 ppm and then remains almost constant. The results
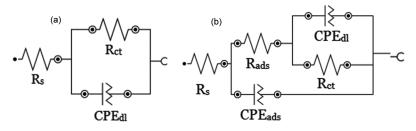

Fig. 4 — The electrochemical equivalent circuit used to fit the data of EIS experiment for the corrosion of carbon steel in 0.5 M HCl solution in theabsence (a) and presence of AO (b).

Table 3 — EIS parameters for carbon steel in 0.5 M HCl in the absence and presence of various concentrations of AO at 20°C.

AO concentration (ppm)	R_s $(\Omega.cm^2)$	R_{ct} $(\Omega.cm^2)$	CPE_{dl}		C_{dl} $(\mu F cm^{-2})$	R_{ads} $(\Omega.cm^2)$	$\eta\%$
			$Y_0(\mu\Omega^{-1} cm^{-2})$	n			
Blank	7.11	74.20	379.7	0.832	184.63	------	------
5.0	4.69	173.56	152.5	0.808	64.49	56.31	67.72
10.0	4.63	208.08	123.4	0.803	50.20	65.64	72.89
20.0	4.72	257.29	114.0	0.804	48.27	67.79	77.18
50.0	5.04	261.64	110.7	0.801	45.91	74.12	77.90
100.0	5.49	264.43	107.3	0.801	44.33	78.27	78.35

obtained from EIS are in agreement with that obtained from polarization test.

Compared with other dyes such as methyl green[13], crystal violet[14] and methyl orange[15], AO has more inhibition performance for carbon steel in HCl solution as depicted in Table 4.

Weight loss measurements

Corrosion rate and inhibition efficiency obtained from CS weight loss measurements in 0.5 M HCl solution without AO and in the presence of different concentrations of AO at 20 °Care given in Table 5.

Table 4 — Comparison of inhibition efficiency of AO with some other dyes

Dye	Concentration	Aggressive medium	$\eta\%$	Ref.
Methylene blue	$5\ mM$	$H_2SO_4\ 2\ M$	61.54	[11]
Methyl green	$1 \times 10^{-5}M$	HCl 1 M	33.3	[13]
Crystal violet	$1 \times 10^{-5}M$	HCl 1M	23.3	[14]
Methyl orange	180 ppm	Well water	12	[15]
Acridine orange	20 ppm	HCl 0.5 M	80.6	This work

Table 5 — CS weight loss data in 0.5 M HCl in the absence and presence of AO at various concentrations for 24 h at 20 °C.

AO concentration (ppm)	Average CR (mpy)	$\eta\%$
Blank	128.12	-----
5.0	98.53	23.10
10.0	30.77	75.98
20.0	25.29	80.26
50.0	20.23	84.21
100.0	23.60	81.58

The results show that with increasing AO concentration, corrosion rate decreases and inhibition efficiency increases. The highest $\eta\%$ was obtained at a concentration of 50 ppm. Comparing the data listed in Table 5 with, it is clear that the results of the potentiodynamic polarization experiments and the weight loss measurements are in agreement with each other and indicate the acceptable accuracy of the results of both types of experiments. Slight differences between the results of the two methods can be ascribe to average corrosion rate measurement as well as the longer test duration in the weight loss experiment, while in the polarization method, the instantaneous corrosion rate is measured[32].

Effect of temperature

Analysis of the dependence of the inhibition efficiency on temperature, as well as the comparison of corrosion activation energies in the absence and presence of inhibitor, provides facts about the possible mechanism of inhibitor adsorption on the metal surface[33]. The effects of temperature on the reaction of metal and corrosive agents in the inhibited environment is very complex, because many changes occur on the metal surface such as rapid etching and adsorption of the inhibitor, and the inhibitor itself may undergo decomposition and/or rearrangement[32].

In order to evaluate the effect of temperature on corrosion rate, Tafel polarization curves of A105 steel sample were recorded in 0.5 M HCl solution at 20, 40, and 60 °C in the absence and presence of different concentrations of AO inhibitor. The polarization plots presented in Figure 5 reveal that for all the studied
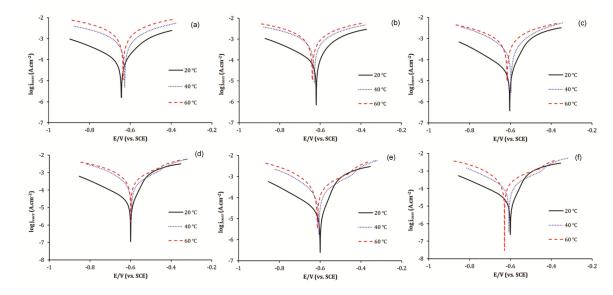

Fig. 5 — Tafel polarization curves of carbon steel in 0.5 HCl M solution at 20, 40 and 60 °C in the absence of the inhibitor (a), and in the presence of 5 (b), 10 (c), 20 (d), 50 (e) and 100 ppm (f) of AO.

concentrations the polarization curves have shifted to higher currents with increasing temperature. Table 6 presents the data derived from polarization tests. It is clear from this table that with increasing temperature, the corrosion potential has shifted to more positive values and the AO behaves as a mixed type inhibitor. The table also demonstrate that the corrosion rate increased with temperature. This is due to the acceleration of all processes involved in corrosion such as electrochemical, chemical, and mass transfer with increasing temperature[34]. Changes in inhibition efficiency with AO concentration for all temperatures show almost same trend; the inhibition efficiency increased with increasing AO concentration and finally remained constant. In addition, with increasing temperature, the inhibition efficiency has also increased. According to the literature[34-36], increasing the inhibition efficiency with increasing temperature can be attributed to the chemical adsorption of inhibitor molecules on the metal surface. Considering the molecular structure of acridine orange (Figure 1), it can be said that the probability of changing the spatial arrangement of methyl groups located on two lateral nitrogen atoms increases with increasing temperature, resulting in increasing the possibility of AO molecule approaching the steel surface and electron transfer from N atoms of AO to Fe atoms of steel.

Bouyanzer et al.[37] and de Souza et al.[38] have described the increase in inhibition efficiency with temperature as specific interactions between the steel surface and the inhibitor. Ivanov[39] has attributed this increase to a change in the nature of adsorption. Accordingly, the inhibitor is physically adsorbed at lower temperatures, while chemisorption of the inhibitor is favourable at higher temperatures. Noor et al.[40] also suggested that with increasing temperature, some chemical changes occur in the inhibitor molecules, which leads to an increase in electron density in the sites responsible for the adsorption of these molecules, which in turn raises the inhibition efficiency.

Noteworthy conclusions on the mechanism of the inhibitor action can be obtained by comparing apparent activation energy (E_a), both in the presence and absence of the corrosion inhibitor. The values of E_a were calculated using Arrhenius equation[41]:

$$\log j_{corr} = \log A - \frac{E_a}{2.303RT} \qquad \ldots (8)$$

Where, T is the absolute temperature, A is the Arrhenius constant and R is the universal gas constant. The plots of $\log j_{corr}$ versus 1/T without and with inhibitor at 5, 10, 20, 50 and 100 ppm gave straight lines (Fig. 6). The calculated values of E_a in the absence and presence of acridine orange are listed in Table 7.

As can be seen from Table 7, the values of activation energy of inhibited solutions are lower than those of blank solution. The lower values of the E_a obtained in presence of AO compared with those

Table 6 — Results of polarization tests and corrosion rates of carbon steel in 0.5 HCl solution without and with different concentrations of AO at different temperatures

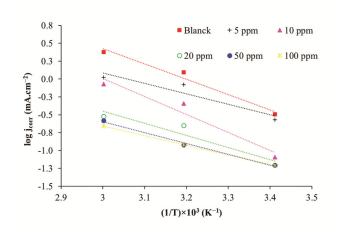| Temperature (°C)	AO concentration (ppm)	E_{corr}/V (vs., SCE)	R_p ($\Omega.cm^{-2}$)	j_{corr} ($mA.cm^{-2}$)	CR (mpy)	$\eta\%$	θ
20	Blank	-0.643	235.88	0.320	146.769	----	----
	5	-0.620	248.72	0.269	123.133	16.04	0.160
	10	-0.603	455.52	0.081	37.009	74.77	0.748
	20	-0.614	549.85	0.062	28.494	80.57	0.806
	50	-0.601	571.69	0.062	28.487	80.58	0.806
	100	-0.601	590.28	0.062	28.409	80.63	0.806
40	Blank	-0.627	75.516	1.243	569.850	----	----
	5	-0.629	82.893	0.836	383.069	32.76	0.328
	10	-0.597	106.99	0.456	208.860	63.34	0.633
	20	-0.596	165.22	0.225	103.059	81.91	0.819
	50	-0.606	244.21	0.120	54.926	90.36	0.904
	100	-0.608	322.37	0.120586	55.266	90.30	0.903
60	Blank	-0.635	42.338	2.393	1096.725	----	----
	5	-0.640	60.104	1.051	481.806	56.07	0.561
	10	-0.616	72.572	0.849	389.264	64.51	0.645
	20	-0.599	141.28	0.302	138.275	87.39	0.874
	50	-0.615	145.9	0.262	119.897	89.07	0.891
	100	-0.629	170	0.2194	100.553	90.83	0.908

Fig. 6 — Arrhenius plots of A105 carbon steel in 0.5 M HCl medium in the absence and presence of various concentrations of AO.

Table 7 — Thermodynamic parameters of the AO adsorptionon carbon steel surface in 0.5 M HCl solution at different temperatures.

AO concentration (ppm)	E_a(kJ $\overline{\mathrm{mol}}$)	ΔH_a^0 (kJmol^{-1})	ΔS_a^0 (J mol$^{-1}K^{-1}$)
Blank	41.08	38.49	-122.25
5	28.05	27.99	-158.61
10	48.19	48.14	-99.66
20	32.45	32.38	-155.69
50	30.46	29.03	-168.53
100	25.66	25.61	-179.97

obtained in its absence can be attributed to its chemisorption on the carbon steel surface[42, 26].

The standard enthalpy of activation (ΔH_a^0) and the standard entropy of activation (ΔS_a^0) for the corrosion of carbon steel were calculated using the following equation:

$$j_{corr} = \frac{RT}{Nh}\exp\left(\frac{\Delta S_a^0}{R}\right)\exp\left(-\frac{\Delta H_a^0}{RT}\right) \qquad \dots(9)$$

where h is Planck's constant, N is Avagadro's number and the other terms have usual meaning. Fig. 7 shows plots of $\log(j_{corr}/T)$ vs. $1/T$. Straight lines are obtained with a slope of $\frac{-\Delta H_a^0}{2.303}$R and an intercept of $[\{\log\left(\frac{R}{Nh}\right)+\left(\frac{\Delta S_a^0}{2.303R}\right)\}]$. The calculated values of $\Delta S_a^0$and ΔH_a^0in the absence and presence of different concentration of AO are listed in Table 7. The values of E_a and ΔH_a^0 should ideally be equal for a chemical reaction in electrolytic solutions[41]. Here, the values of these quantities are approximately equal. Positive values of ΔH_a^0 in the absence and presence of
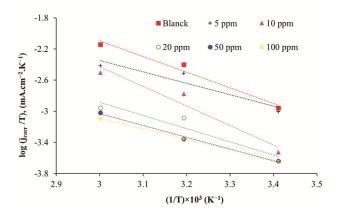

Fig. 7 — Transition-state plots for carbon steel corrosion rates in 0.5 M HCl solution in absence and presence of 5, 10, 20, 50 and 100 ppm of AO.

inhibitor imply that the steel dissolution has an end other micnature.

The values $\Delta S_a^0$are negative both in the absence and presence of the inhibitor. Large and negative values of ΔS_a^0indicate that the activated complex in the rate-determining step includes an association rather than a dissociation step, which means that there is a decrease in disordering on going from the reactants to the activated complex[26].

On the other hand, with increasing inhibitor concentration, the values of entropies have become more negative, indicating that the activated complex is more ordered in the presence of AO[41]. In blank solution, the activated complex can be considered as$Fe-H_2O$ which decomposes during corrosion to produce Fe^{2+}, H_2, and OH^{-}[43]. In the presence of inhibitor, $Fe-H_2O$is replaced by Fe-inhibitor complex. Compared to the blank solution, $\Delta S_a^0$is shifted to more negative values on the addition of inhibitor, indicating that the Fe-inhibitor complex is more ordered than the $Fe-H_2O$complex[41].

Adsorption isotherm

The mechanism of adsorption and interaction between inhibitor and the metallic surface can be characterized by adsorption isotherms[44]. In order to evaluate the adsorption process of AO on the carbon steel surface, Langmuir, Temkin and Freundlich adsorption isotherms were investigated. The correlation coefficient, R^2, was used to choose the isotherm that best fit experimental data. The best fit is obtained with Langmuir isotherm. Figure 8 shows the Langmuir isotherm diagrams obtained at different temperatures. The Langmuir isotherm can be expressed by the following equation[26]:
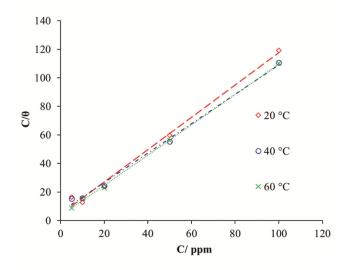
Fig. 8 — Langmuir adsorption isotherm for carbon steel in 0.5 M HCl containing various concentration of AO at 20, 40 and 60 °C.

Table 8 — Thermodynamic data of inhibitor adsorption on steel surface in 0.5 M HCl solution obtained from Langmuir isotherm

T (K)	K_{ads} $(L.mg^{-1})$	K_{ads} $(L.mol^{-1})$	$\Delta G^0_{ads}(J.mol^{-1})$
293	0.226	6.03×10^4	−37.22
313	0.161	4.30×10^4	−36.38
333	0.298	7.94×10^4	−37.90

$$\frac{C_{inh}}{\theta} = \frac{1}{K_{ads}} + C_{inh} \qquad \dots (10)$$

where, K_{ads} is the equilibrium constant of the adsorption process, C_{inh} is the inhibitor concentration and θ is the surface coverage. The θ values calculated using potentiodynamic polarization data at 20, 40 and 60 °C for carbon steel in 0.5 M HCl with various concentrations of AO. The K_{ads} values can be calculated from the intercept lines on the C/θ-axis. The standard free energy of adsorption, ΔG^0_{ads}, is derived from the K_{ads} by the following equation:

$$K_{ads} = \frac{1}{55.5} e^{-\left(\frac{\Delta G^0_{ads}}{RT}\right)} \qquad \dots (11)$$

Table 8 presents the thermodynamic parameters corresponds to the adsorption of AO on the steel surface in the 0.5 HCl solution derived from the Langmuir isotherm. High values of the K_{ads} imply the ease of inhibitor molecules adsorption onto the steel surface, and the negative sign of ΔG^0_{ads} indicates that the adsorption process is spontaneous.

In addition, high values of ΔG^0_{ads} can mean that the tendency of inhibitor molecules to be adsorbed on the steel surface is very high. According to the literature[26], since the calculated values of ΔG^0_{ads} are less than −40 $kJmol^{-1}$ thus the predominant mechanism for adsorption of AO molecules on the steel surface can be considered as physisorption, meaning electrostatic interactions exist between the inhibitor and the charged metal surface.

Conclusion

The efficiency of acridine orange as a low cost corrosion inhibitor for A105 carbon steel in 0.5 HCl solution has been investigated using electrochemical potentiodynamic polarization and EIS and weight loss measurements. The results of all three methods have shown that the inhibition efficiency increases with increasing AO concentration, due to the formation of a thicker protective film on the metal surface. It has also been found that AO in HCl medium acts as a mixed-type inhibitor. The corrosion rates and inhibition efficiencies obtained from the three methods have in good agreement. This agreement between the three independent methods confirms the validity of the results. Results of temperature effect study have shown that the inhibition efficiency increases with temperature. One of the main influencing factor in increasing the inhibition efficiency with temperature is the change in the spatial arrangement of the inhibitor molecule due to heat. Assessment of the thermodynamic and kinetic parameters have revealed that positive values of ΔH^0_a indicate the difficulty of metal dissolution and negative values of ΔS^0_a indicate an association of activated complex in the rate-determining step. In addition, it was been found that the adsorption process of AO on the steel surface in this medium obeys the Langmuir isotherm and the adsorption process is performed spontaneously and has a physisorption mechanism.

References
1   Khadom A A, Abd A N & N A Ahmed, *South Afr J Chem Eng*, 25 (2018) 13.
2   Goyal M, Kumar S, Bahadur I, Verma C & Ebenso E E, *J MolLiq*, 256 (2018) 565.
3   Sığırcık G, Yildirim D & Tüken T, *Corros Sci*, 120 (2017) 184.
4   Ameer M A & Fekry A M, *Int J Hydrogen Energy*, 35 (2010) 11387.

5   Yavari Z, Nematiyan S, Saraveni H & Noroozifar M, *Indian J Chem Technol*, 27 (2020) 227.
6   Tang L B, Mu G N & Liu G H, *Corros Sci*, 45 (2003) 2251.
7   Ebenso E E & Oguzie E E, *Mater Lett*, 59 (2005) 2163.
8   Onen A I, Maitera O N, Joseph J & Ebenso E E, *Int J Electrochem Sci*, 6 (2011) 2884.
9   Oguzie E E, *Mater Chem Phys*, 87 (2004) 212.
10 Oguzie E E & Ebenso E E, *Pigment Resin Technol*, 35 (2006) 30.
11 Oguzie E E, Onuoha G N & Onuchuku A I, *Mater Chem Phys*, 89 (2005) 305.
12 Oguzie E E, *Mater Lett*, 59 (2005) 1076.
13 Oguzie E, Akalezi C & Enenebeaku C, *Pigment Resin Technol*, 38 (2009) 359.
14 Oguzie E E, Njoku V O, Enenebeaku C K, Akalezi C O & Obi C, *Corros Sci*, 50 (2008) 3480.
15 Sathiyabama J, Rajendran S, Solvi J A & Amalraj A J, *Indian J Chem Technol*, 15 (2008) 462.
16 Li X, Deng S & Fu H, *Corros Sci*, 52 (2010) 3413.
17 Deng S D, Li X H & Fu H, *J Appl Electrochem*, 40 (2010) 2107.
18 Deng S D, Li X H & Fu H, *Corros Sci*, 53 (2011) 3596.
19 Deng S D, Li X H & Fu H, *Corros Sci*, 53 (2011) 760.
20 Jiao J, Shen J, Wang L, Xie Z, Xia C & Xin X, *Colloids Surf A*, 545 (2018) 8.
21 Bringas J E, *Handbook of Comparative World Steel Standards*, 3rd Edn, (ASTM International Publication, West Conshohocken), (2004) 275.
22 Hazra S, Mukhopadhyay S & Adhikari U, *Indian J Chem Technol*, 27 (2020) 395.
23 Arellanes-Lozada P, Díaz-Jiménez V, Hernández-Cocoletzi H, Nava N, Olivares-Xometl O & Likhanova N V, *Corros Sci*, 175 (2020) 108888.
24 Behpour M, Ghoreishi S M, Soltani N, Salavati-Niasari M, Hamadanian M & Gandomi A, *Corros Sci*, 50 (2008) 2172.
25 Caldona E B, Zhang M, Liang G, Hollis T K, Webster C E, JrD W S & Wipf D O, *J Electroanal Chem*, 880 (2021) 114858.
26 Soltani N, Tavakkoli N, Khayat K M, Jalali M R & Mosavizade A, *Corros Sci*, 62 (2012) 122.
27 Wang B, Du M, Zhang J, Li C, Liu J, Liu H, Li R & Li Z, *RSC Adv*, 9 (2019) 36546.
28 Li D, Zhang P, Guo X, Zhao X & Xu Y, *RSC Adv*, 9 (2019) 40997.
29 Hsissou R, About S, Seghiri R, Rehioui M, Berisha A, Erramli H, Assouag M & Elharfi A, *J Mater Res Technol*, 9 (2020) 2691.
30 Yadav D K, Quraishi M A & Maiti B, *Corros Sci*, 55 (2012) 254.
31 Singh A, Ansari K R, Xu X, Sun Z, Kumar A & Lin Y, *Sci Rep*, 7 (2017) 1.
32 Bentiss F, Lebrini M & Lagreneé M, *Corros Sci*, 47 (2005) 2915.
33 Bahrami M J, Hosseini S M A & Pilvar P, *Corros Sci*, 52 (2010) 2793.
34 Okafor P C, Liu X & Zheng Y G, *Corros Sci*, 51 (2009) 761.
35 Oguzie E E, *Corros Sci*, 50 (2008) 2993.
36 Satapathy A K, Gunasekaran G, Sahoo S C, Amit K & Rodrigues P V, *Corros Sci*, 51 (2009) 2848.
37 Bouyanzer A & Hammouti B, *Pigment Resin Technol*, 33 (2004) 287.
38 de Souza F S, Spinelli A, *Corros Sci*, 51 (2009) 642.
39 Ivanov E S, *Metallurgy*, (1986) 175.
40 Noor E A & Al-Moubaraki A H, *Mater Chem Phys*, 110 (2008) 145.
41 Mourya P, Banerjee S & Singh M M, *Corros Sci*, 85 (2014) 352.
42 Behpour M, Ghoreishi S M, Khayat Kashani M & Soltani N, *Mater Corros*, 60 (2009) 895.
43 Obot I B & Obi-Egbedi N O, *Corros Sci*, 52 (2010) 198.
44 Farhadian A, Rahimi A, Safaei N, Shaabani A, Abdouss M & Alavi A, *Corros Sci*, 175 (2020) 108871.